SM and BSM $\gamma\gamma$->VV in diffractive photon fusion at the LHC

Rick Sandeepan Gupta

(IFAE, Barcelona)

Diffractive photon fusion to $\gamma\gamma/ZZ/WW$

- Experimentally $\gamma\gamma VV$ couplings can be cleanly measured in the process:

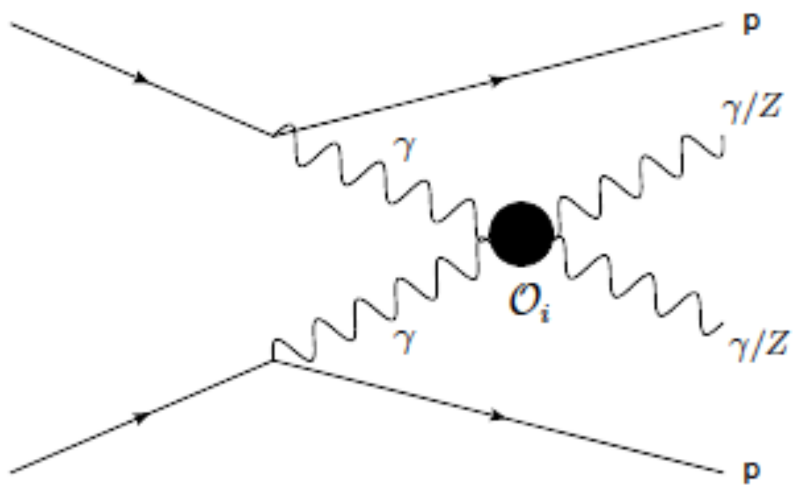

- Intact protons can be detected by very forward proton detectors to be installed by ATLAS and CMS.

Very forward detectors

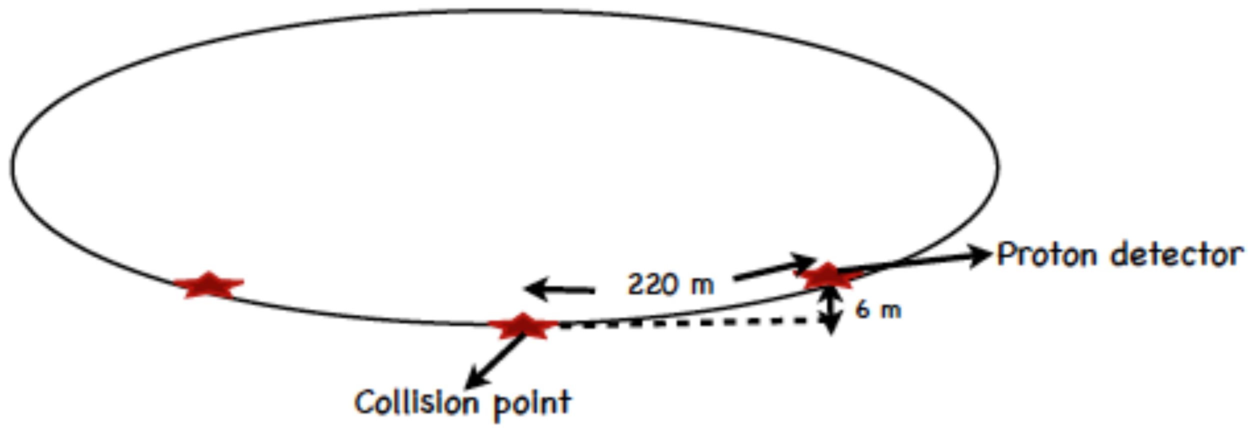

- Final state protons in diffractive processes are scattered at small angles. To detect such protons very forward detectors (220 m and 420 m from the interaction point) have been proposed for both ATLAS and CMS.

Very forward detectors

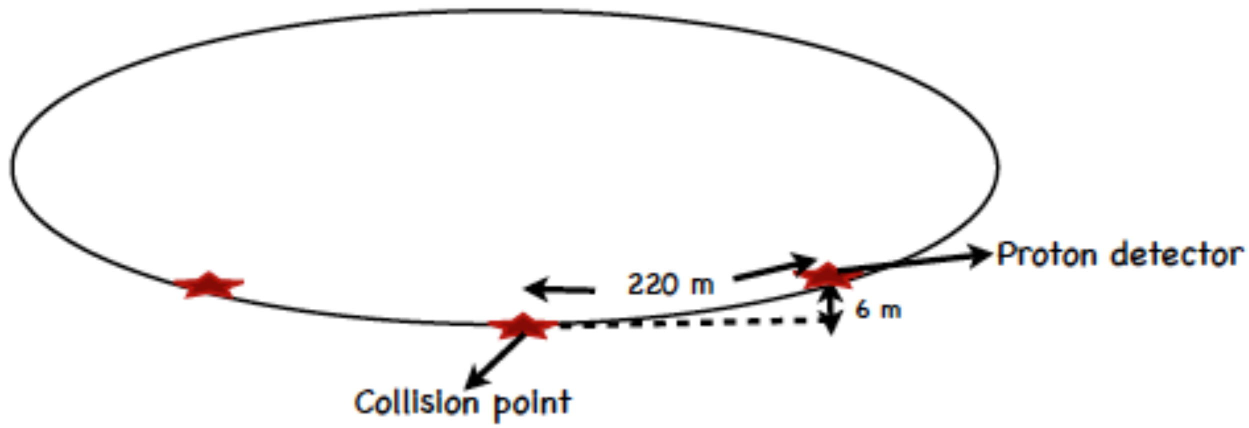

- The LHC magnets continue to curve the protons along the beam.

Very forward detectors

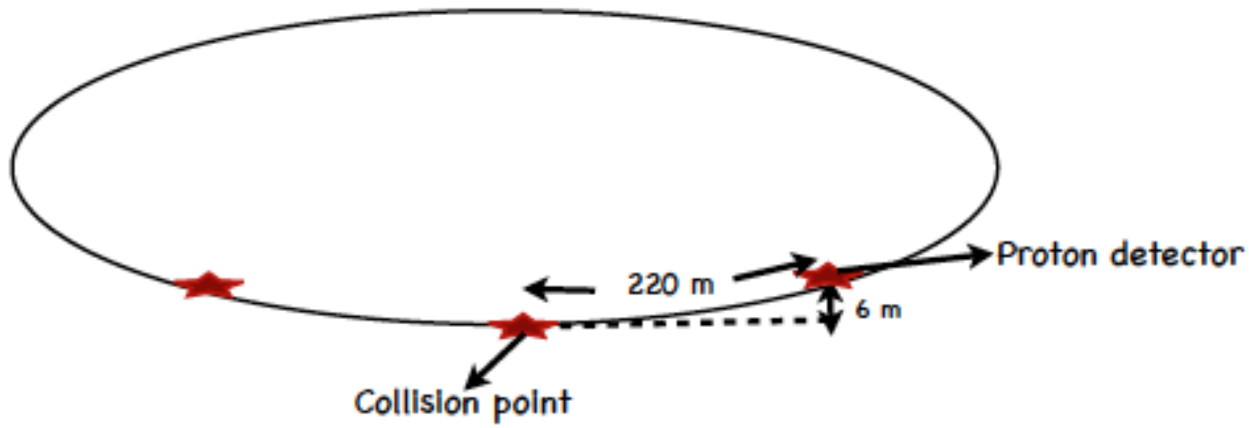

- Particles other than protons would never be detected in these detectors as they have a different cyclotron radius. Thus these detectors effectively use the LHC magnets as a spectrometer.

Equivalent photon approximation

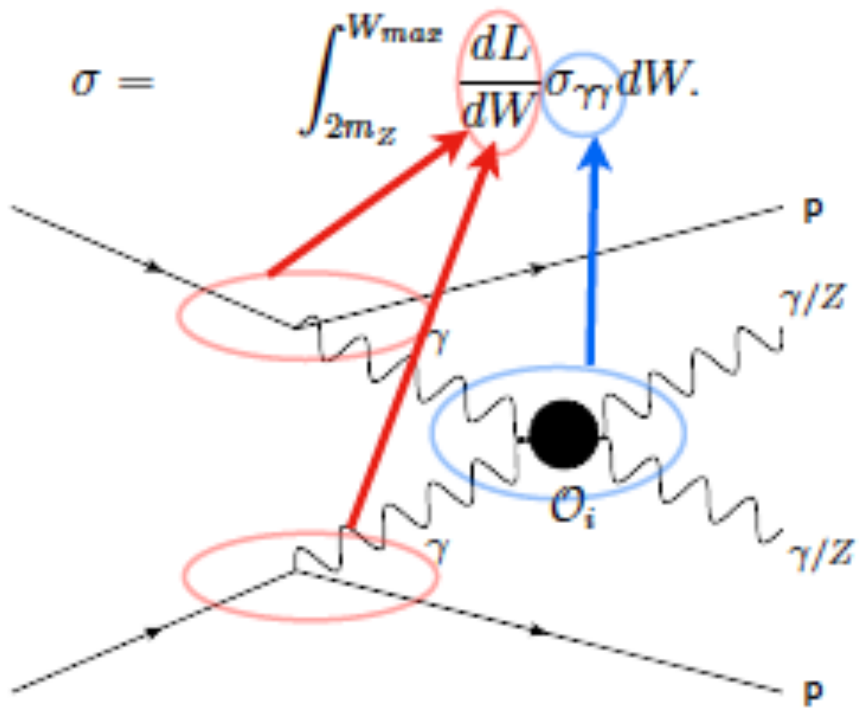

- The photons to a very good approximation are on-shell. The cross-section can thus be factorized into two parts as shown above.

Equivalent photon approximation

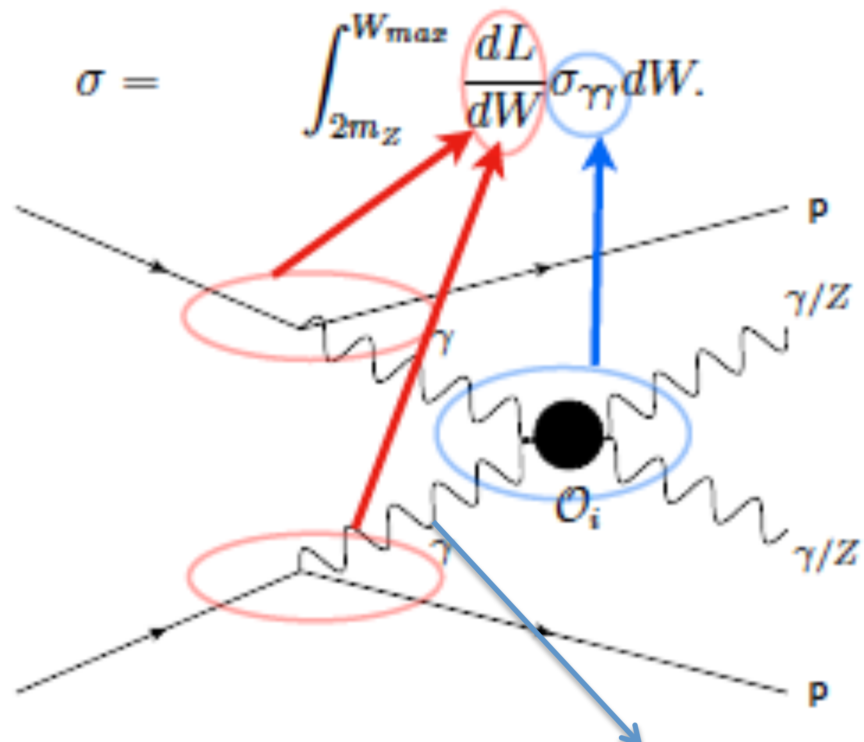

- Physically this happens because of the $1/q_i^2$ in the photon propagators. The amplitude thus peaks for that is on shell photons ($|q_i^2| \to 0$).

Equivalent photon approximation

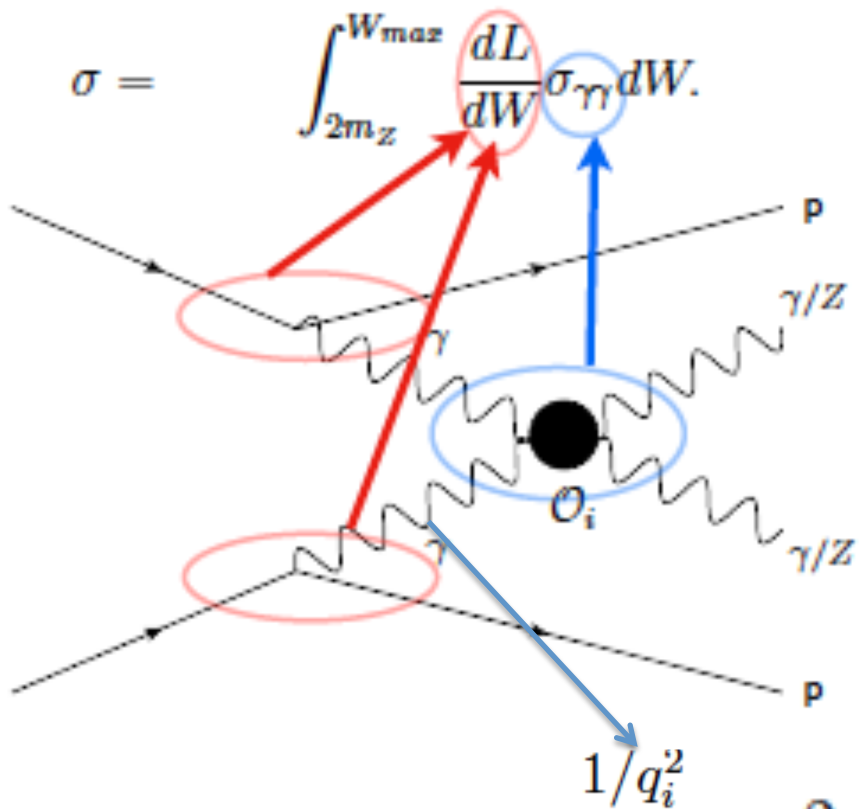

- Kinematics implies that small photon q_i^2 is related to small proton *pT*. This is why protons are so forward.

Equivalent photon approximation: the luminosity function

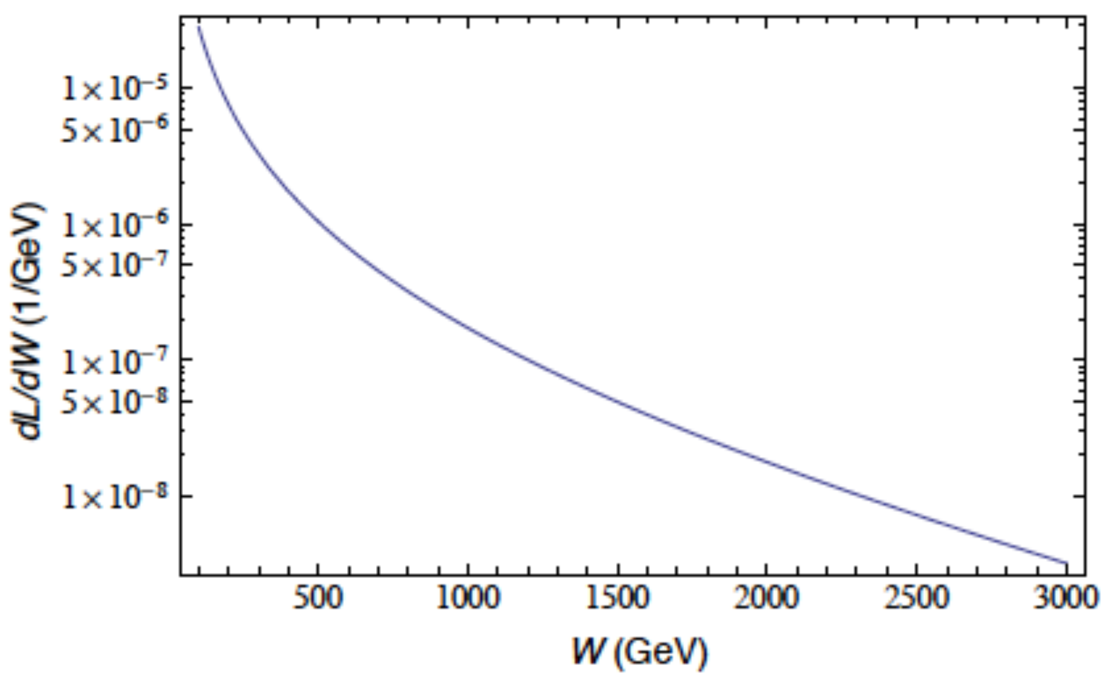

Background: Double Pomeron Exchange

- Pomerons are neutral colour singlet bound states in QCD.
- A proton can elastically emit a pomeron.
- Two pomerons can interact to produce a final state. This usually also produces pomeron remnants.

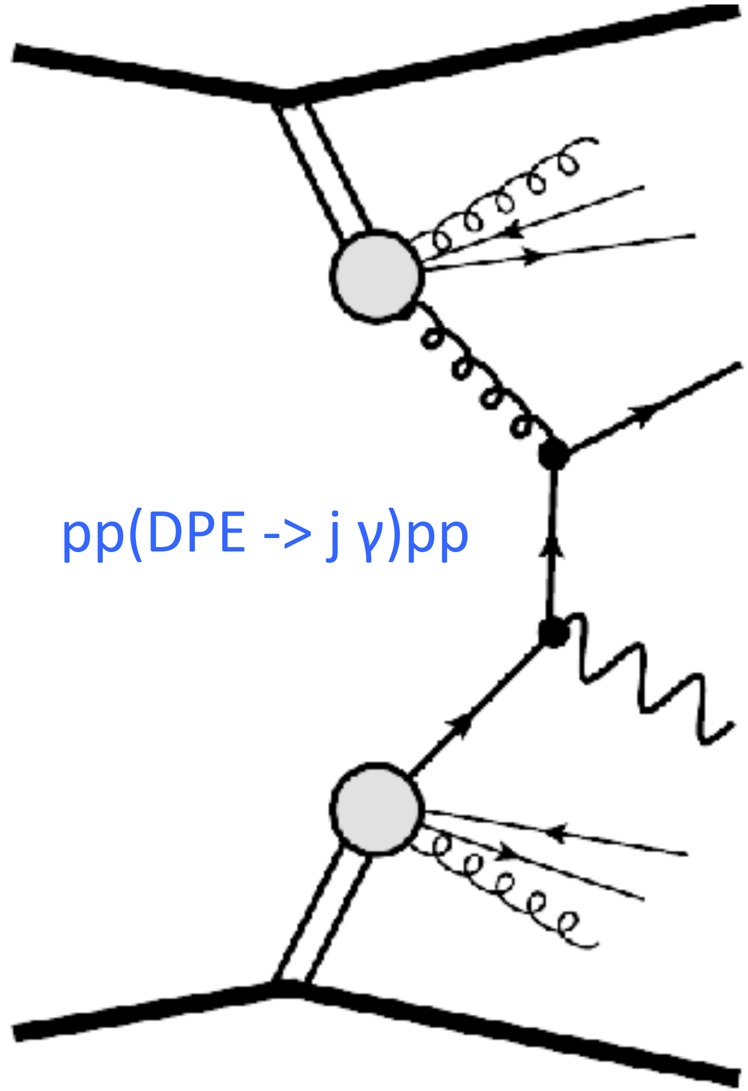

pp(DPE -> j γ)pp

The SM $\gamma\gamma WW$ cross-section

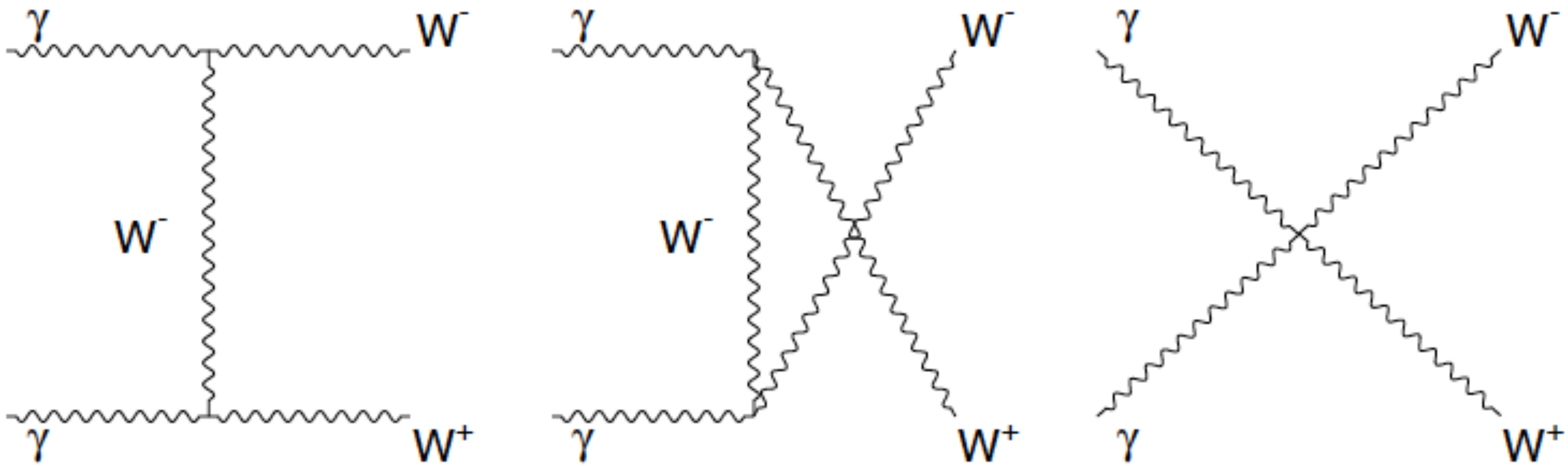

• We need to find the hard cross-sections and convolute with the photon luminosity function. We finally find:

(Chapon, Royon and Kepka 2009)

process	total cross section
$\gamma\gamma \to WW$	96.5 fb
$\gamma\gamma \to ll\ (p_T^{lep1} > 5\,\text{GeV})$	39.4 pb
DPE$\to ll$	7.4 pb
DPE$\to WW$	8.1 fb

(these cross-sections include protons in the initial and final states and the BR to leptons)

The SM $\gamma\gamma WW$ cross-section

cut / process	$\gamma\gamma \to ee$	$\gamma\gamma \to \mu\mu$	$\gamma\gamma \to \tau\tau$	DPE$\to ll$	DPE$\to WW$	$\gamma\gamma \to WW$
gen. $p_T^{lep1} > 5\,\mathrm{GeV}$	364500	364500	337500	295200	530	1198
$p_T^{lep1,2} > 10\,\mathrm{GeV}$	24896	25547	177	17931	8.8	95
$0.0015 < \xi < 0.15$	10398	10535	126	11487	5.9	89
$\not{E}_T > 20\,\mathrm{GeV}$	0	0.86	14	33	4.7	78
$W > 160\,\mathrm{GeV}$	0	0.86	8.3	33	4.7	78
$\Delta\phi < 2.7$	0	0	0	14	3.8	61
$p_T^{lep} > 25\,\mathrm{GeV}$	0	0	0	7.5	3.5	58
$W < 500$	0	0	0	1.0	0.67	51
$\xi < 0.1$	0	0	0	0.85	0.54	47
$\xi < 0.05$	0	0	0	0.40	0.25	32

Background rejection with 30 /fb data.

(Chapon, Royon and Kepka 2009)

5σ discovery can be achieved with only 5/fb!

The SM $\gamma\gamma ZZ$ cross-section

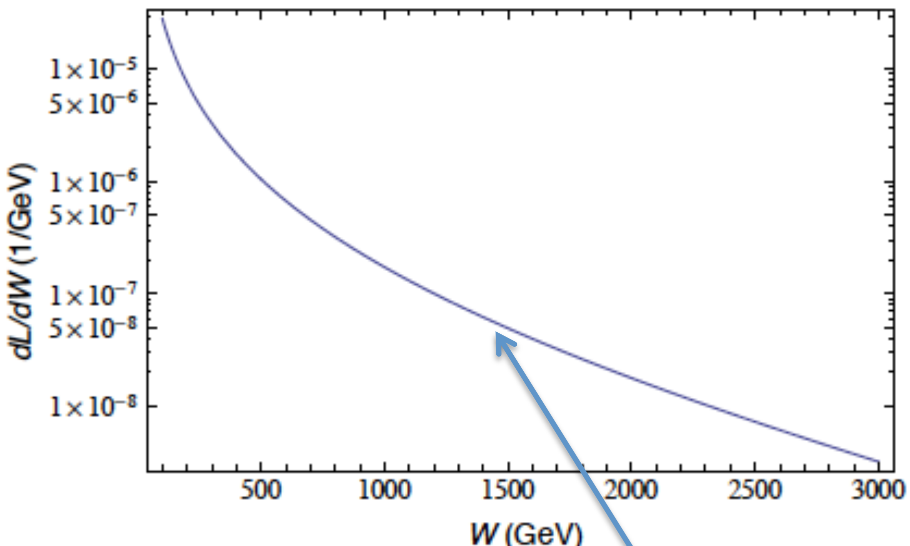

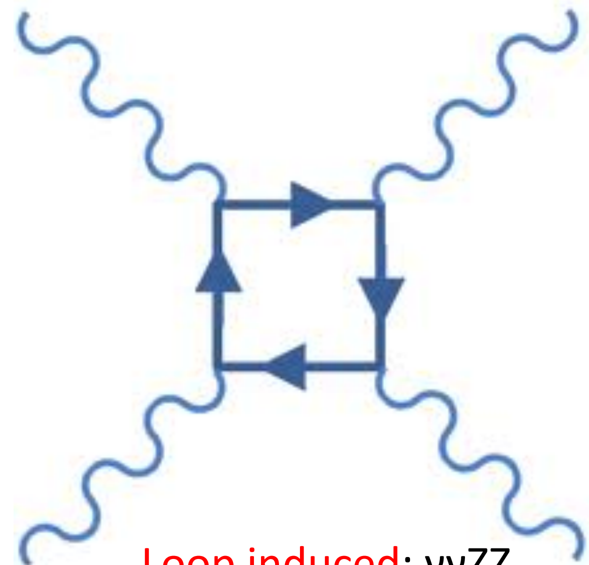

Loop induced: γγZZ much smaller cross-section than γγWW

$$\sigma = S^2_{QED} \int_{2M_Z}^{2100} \frac{dL}{d\tau}\sigma_{\gamma\gamma} d\tau \approx 0.9 \times 300 \int_{2M_Z}^{2100} \frac{dL}{d\tau} d\tau \approx 0.1 \text{ fb},$$

The SM $\gamma\gamma ZZ$ cross-section

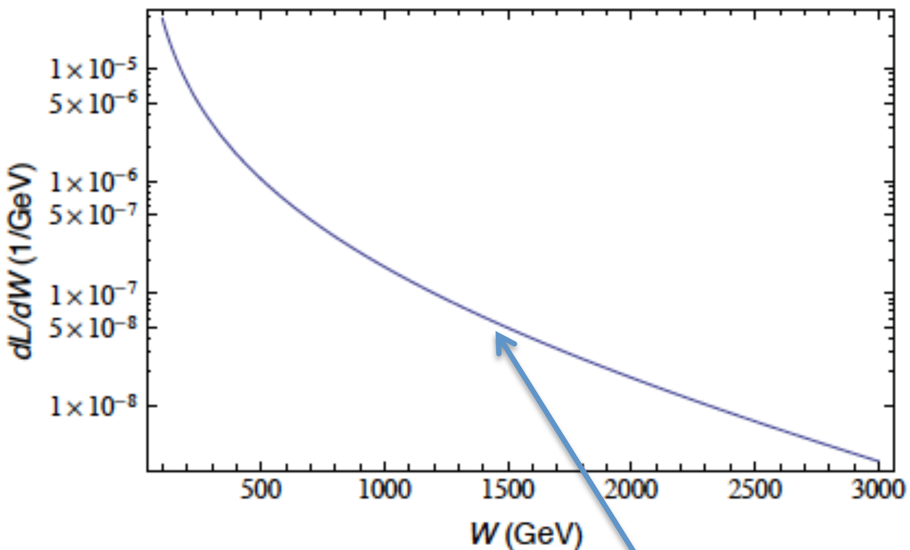

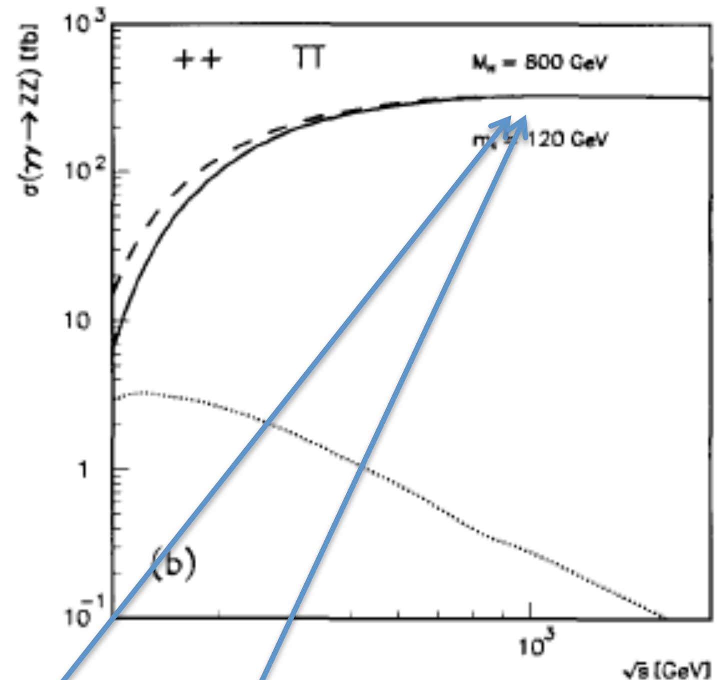

(Jikia, 1993)

$$\sigma = S^2_{QED} \int_{2M_Z}^{2100} \frac{dL}{d\tau} \sigma_{\gamma\gamma} d\tau \approx 0.9 \times 300 \int_{2M_Z}^{2100} \frac{dL}{d\tau} d\tau \approx 0.1 \text{ fb},$$

(excluding Z branching ratios)

The SM *γγγγ* cross-section

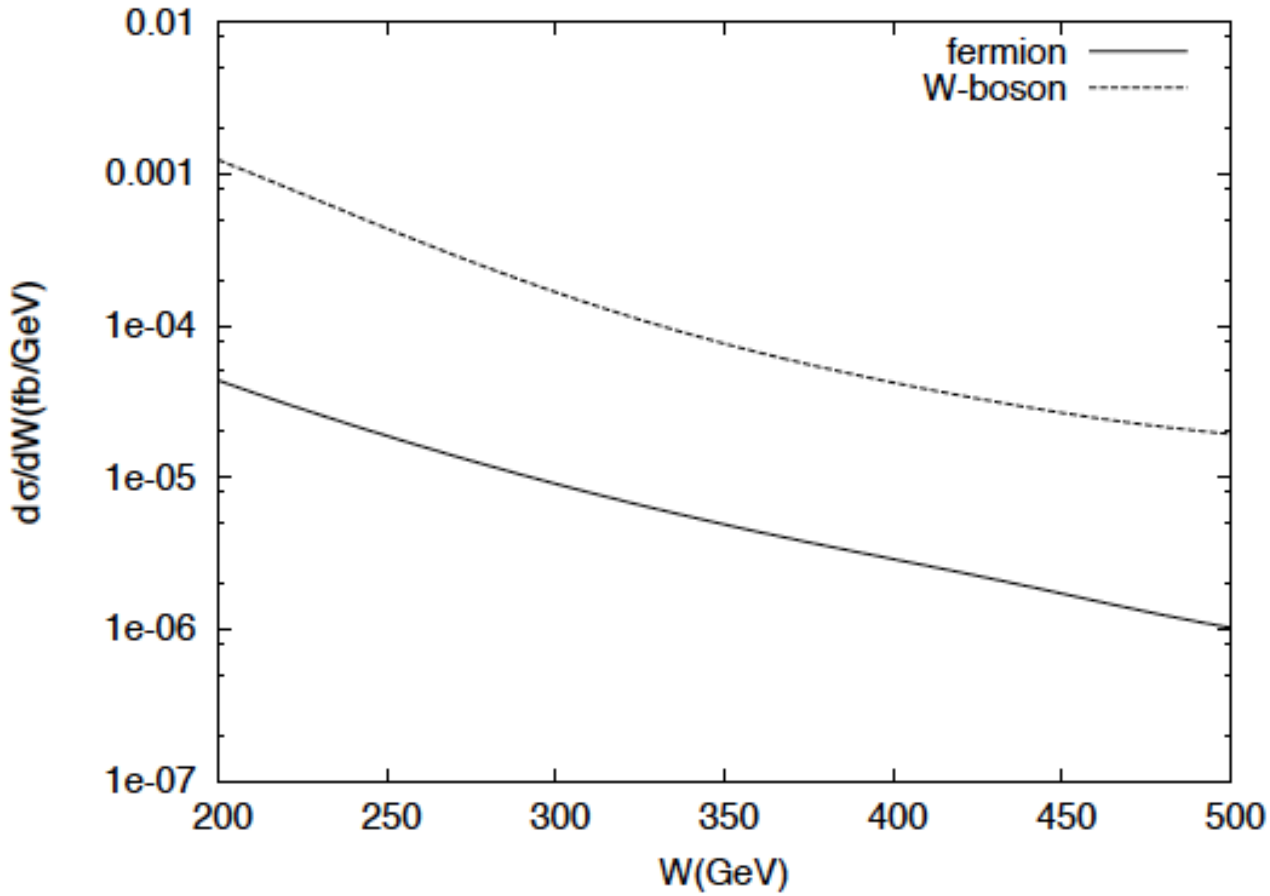

(Atag et al 2010)

The pp (γγ->γγ)pp cross-section.

The total cross-section is of the order of 0.01 fb

Background: Double Pomeron Exchange

- pp(DPE -> γγ/ZZ)pp processes have cross section of the order of a few femtobarns.

- Both pp(γγ -> γγ)pp and pp(γγ -> ZZ)pp are thus very challenging to see at the LHC if there are no BSM contributions.

γγγγ, γγZZ beyond the SM

$$
\begin{aligned}
\mathcal{L}_{QNGC} \;=\;& \frac{c_1}{\Lambda^4} D_\mu\Phi^\dagger D^\mu\Phi D_\nu\Phi^\dagger D^\nu\Phi + \frac{c_2}{\Lambda^4} D_\mu\Phi^\dagger D_\nu\Phi D^\mu\Phi^\dagger D^\nu\Phi + \frac{c_3}{\Lambda^4} D_\rho\Phi^\dagger D^\rho\Phi B_{\mu\nu}B^{\mu\nu} \\
&+ \frac{c_4}{\Lambda^4} D_\rho\Phi^\dagger D^\rho\Phi W^I_{\mu\nu}W^{I\mu\nu} + \frac{c_5}{\Lambda^4} D_\rho\Phi^\dagger\sigma^I D^\rho\Phi B_{\mu\nu}W^{I\mu\nu} + \frac{c_6}{\Lambda^4} D_\rho\Phi^\dagger D^\nu\Phi B_{\mu\nu}B^{\mu\rho} \\
&+ \frac{c_7}{\Lambda^4} D_\rho\Phi^\dagger D^\nu\Phi W^I_{\mu\nu}W^{I\mu\rho} + \frac{c_8}{\Lambda^4} B_{\rho\sigma}B^{\rho\sigma}B_{\mu\nu}B^{\mu\nu} + \frac{c_9}{\Lambda^4} W^I_{\rho\sigma}W^{I\rho\sigma}W^J_{\mu\nu}W^{J\mu\nu} \\
&+ \frac{c_{10}}{\Lambda^4} W^I_{\rho\sigma}W^{J\rho\sigma}W^I_{\mu\nu}W^{J\mu\nu} + \frac{c_{11}}{\Lambda^4} B_{\rho\sigma}B^{\rho\sigma}W^I_{\mu\nu}W^{I\mu\nu} + \frac{c_{12}}{\Lambda^4} B_{\rho\sigma}W^{I\rho\sigma}B_{\mu\nu}W^{I\mu\nu} \\
&+ \frac{c_{13}}{\Lambda^4} B_{\rho\sigma}B^{\sigma\nu}B_{\mu\nu}B^{\mu\rho} + \frac{c_{14}}{\Lambda^4} W^I_{\rho\sigma}W^{I\sigma\nu}W^J_{\mu\nu}W^{J\mu\rho} + \frac{c_{15}}{\Lambda^4} W^I_{\rho\sigma}W^{J\sigma\nu}W^I_{\mu\nu}W^{J\mu\rho} \\
&+ \frac{c_{16}}{\Lambda^4} B_{\rho\sigma}B^{\sigma\nu}W^I_{\mu\nu}W^{I\mu\rho} + \frac{c_{17}}{\Lambda^4} B_{\rho\sigma}W^{I\sigma\nu}B_{\mu\nu}W^{I\mu\rho}.
\end{aligned}
$$

(RSG, Nov 2011)

- Quartic Neutral Gauge couplings *γγZZ* and *γγZZ* are generated only by dimension 8 operators. Most processes probe dimension 6 operators. These couplings are unique because they can access dimension 8 operators.
- These operators are generated by virtual graviton exchange in extra dimensional theories.

Unitarity bounds and form factors

- Amplitude due to effective operators grow with energy and become unreliable near the cut-off.

$$\mathcal{A}(\gamma\gamma \to Z_T Z_T) \sim a_i \frac{\hat{s}^2}{\Lambda^4}$$
$$\mathcal{A}(\gamma\gamma \to Z_L Z_L) \sim a_i \frac{M_Z^2 \hat{s}}{\Lambda^4} \frac{\hat{s}}{M_Z^2} \sim a_i \frac{\hat{s}^2}{\Lambda^4}$$

The Unitarity bound

- Optical theorem:

$$\begin{aligned}\frac{\mathrm{Im}(\mathcal{M}(\gamma_1\gamma_2\to\gamma_1\gamma_2))}{s} &= \sigma(\gamma_1\gamma_2\to \text{everything}) \\ &= \sigma(\gamma_1\gamma_2\to\gamma(\epsilon_1)\gamma(\epsilon_2)) + \sum_{\epsilon_3,\epsilon_4}\sigma(\gamma_1\gamma_2\to Z(\epsilon_3)Z(\epsilon_4)) \\ &\quad +\Delta\end{aligned}$$

$$\sigma = \frac{\beta_W}{64\pi^2 s}\int d\Omega_{\mathrm{CM}}\,|\mathcal{M}(\gamma_1\gamma_2\to VV)|^2.$$

$$\begin{aligned}\mathcal{M}(\gamma_1\gamma_2\to\gamma_1\gamma_2) &= 16\pi\sum_J(2J+1)b_J P_J(\cos\theta) \\ \mathcal{M}(\gamma_1\gamma_2\to ZZ) &= 16\pi\sum_J(2J+1)a_J P_J(\cos\theta).\end{aligned}$$

$$(\mathrm{Re}(b_l))^2 + \beta\sum_{\epsilon_3,\epsilon_4}|a_l|^2 + \delta_l < \frac{1}{4}.$$

- Amplitudes cannot keep growing with energy!

What this means is that the effective field theory approximation breaks down and the we must include the new interactions and particles that generate the operators in the first place, to obtain the correct amplitude.

Form factors

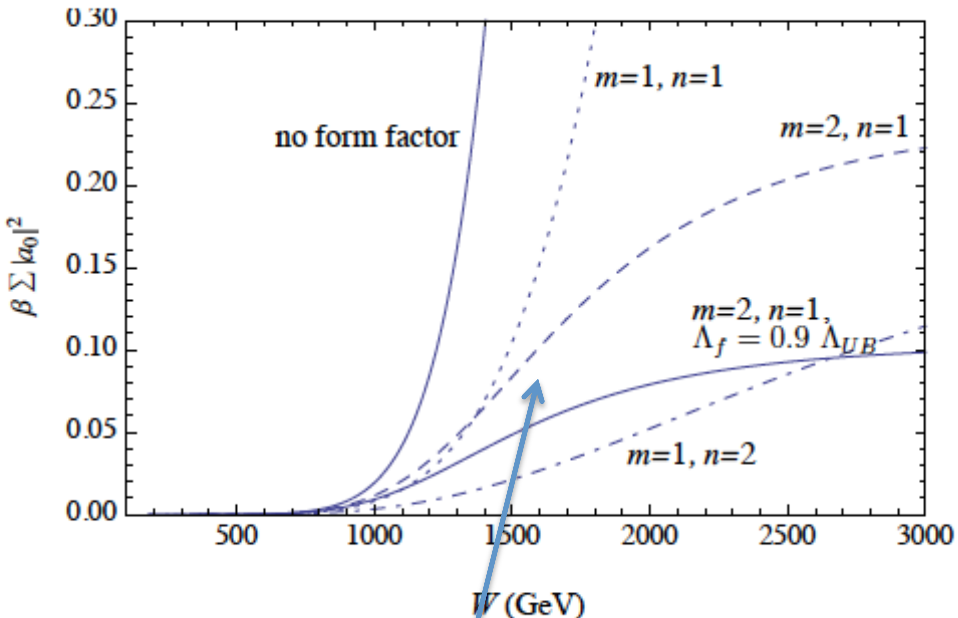

• Form factors solve the problem of amplitudes growing with energy but the choice of the form factor is ambiguous and unphysical.

$$\mathcal{A} \to \mathcal{A}\left(\frac{1}{1+(\hat{s}/\Lambda_f^2)^m}\right)^n$$

• The largest contribution from the BSM signal comes at higher energies. But this is also the most unreliable part !

Form factors

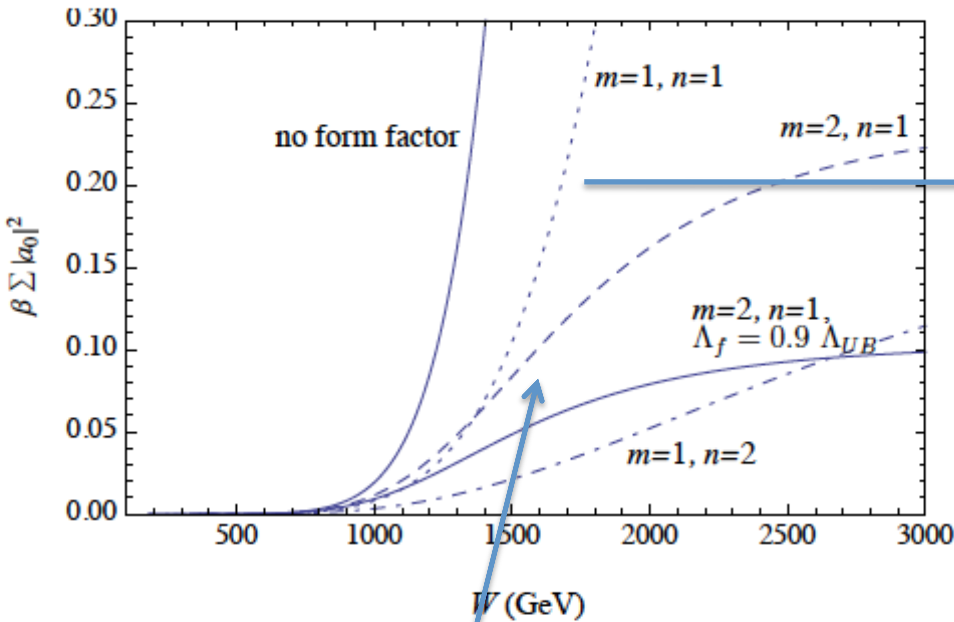

Form factors
must actual unitarize!
Some previous studies
have used very weak
form factors.

• Form factors solve the problem of amplitudes growing with energy but the choice of the form factor is ambiguous and unphysical.

$$\mathcal{A} \to \mathcal{A}\left(\frac{1}{1+(\hat{s}/\Lambda_f^2)^m}\right)^n$$

• The largest contribution from the BSM signal comes at higher energies. But this is also the most unreliable part !

Proposal: physical form factors ?

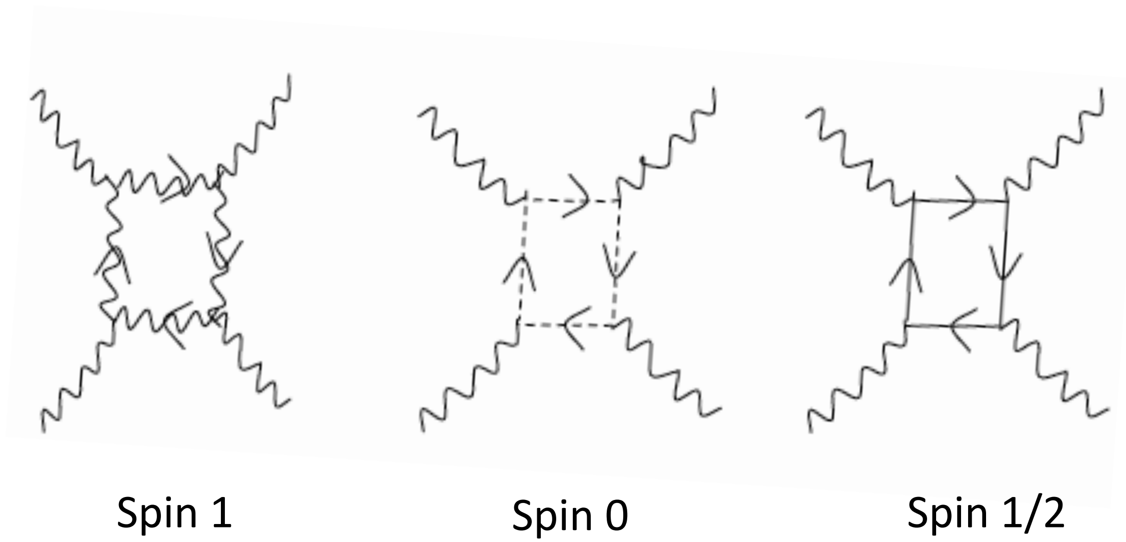

•The massive particles in the loop above give the same amplitude as our operators at low energies:

$$\frac{a_1^{\gamma\gamma}}{\Lambda^4} F_{\mu\nu} F^{\mu\nu} F_{\rho\sigma} F^{\rho\sigma} + \frac{a_2^{\gamma\gamma}}{\Lambda^4} F_{\mu\nu} F^{\mu\rho} F_{\rho\sigma} F^{\sigma\nu}$$

• At energies close to the cut-off, we can deduce a ‘physical’ form factor from each of the above amplitudes.

‘Hard’ cross-sections

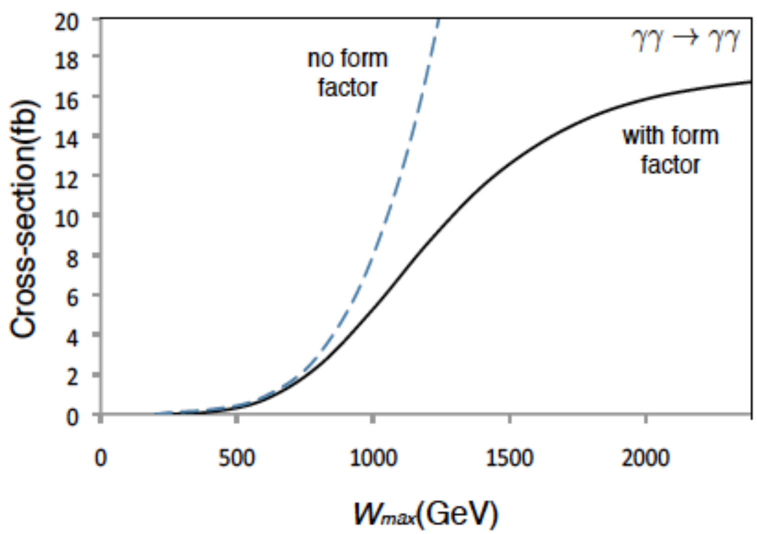

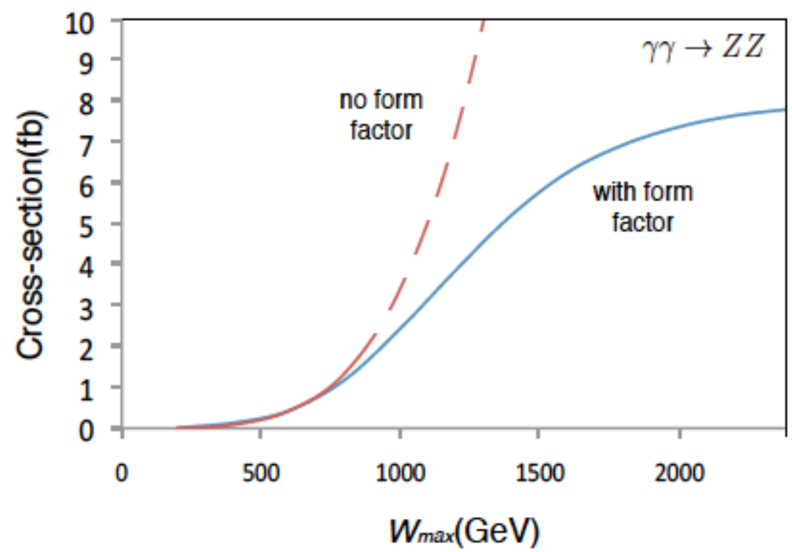

Cross-sections before convoluting with luminosity function taking all couplings equal to unity.
(Form factor used: m=2,n=1)

Results

Couplings	Process	Integrated Luminosity(fb^{-1})	N_{obs}	N_b	Confidence Level(sigma)
Case 1: $(850\ \text{GeV})^{-4}$	$\gamma\gamma \to \gamma\gamma$	1	12.1	0.3	>10
Case 1: $(1.8\ \text{TeV})^{-4}$	$\gamma\gamma \to \gamma\gamma$	300	133.1	82.8	5.2
Case 1: $(850\ \text{GeV})^{-4}$	$\gamma\gamma \to ZZ$	300	7.4(1.9)	1.1(0.3)	4.3(2.1)
Case 1: $(750\ \text{GeV})^{-4}$	$\gamma\gamma \to ZZ$	300	11.4(2.8)	1.1(0.3)	6.0(2.9)
Case 1:$(500\ \text{GeV})^{-4}$	$\gamma\gamma \to ZZ$	300	46.8(11.7)	1.1(0.3)	>10(8.1)
Case 2:$(700\ \text{GeV})^{-4}$	$\gamma\gamma \to ZZ$	300	14.8(3.7)	2.1(0.5)	5.8(3.1)
Case 2:$(500\ \text{GeV})^{-4}$	$\gamma\gamma \to ZZ$	300	51.3(12.8)	2.1(0.5)	8.2(7.7)
Case 3: $\Lambda_T = 1.0$ TeV	$\gamma\gamma \to \gamma\gamma$	1	13.5	0.3	>10
Case 3: $\Lambda_T = 2.4$ TeV	$\gamma\gamma \to \gamma\gamma$	300	118.2	82.8	3.9
Case 3: $\Lambda_T = 900$ GeV	$\gamma\gamma \to ZZ$	300	12.6(3.2)	1.1(0.3)	6.4(3.6)
Case 3: $\Lambda_T = 700$ GeV	$\gamma\gamma \to ZZ$	300	39.6(9.9)	1.1(0.3)	>10(7.1)
Case 4:$(1.9\ \text{TeV})^{-2}$	$\gamma\gamma \to ZZ$	300	5.3(1.3)	1.1(0.3)	3.3(2.1)
Case 4:$(2.2\ \text{TeV})^{-2}$	$\gamma\gamma \to ZZ$	300	3.9(1.0)	1.1(0.3)	2.2(1.1)

Form factor used: *m*=2,*n*=1. The only substantial background is the pp(DPE->γγ/ZZ)pp already discussed.

Huge improvement over previous constraints $-\frac{1}{(69\,\text{GeV})^4} < \frac{a_1^{ZZ}}{\Lambda^4} < \frac{1}{(93\,\text{GeV})^4}$

Λ not necessarily new physics scale

- Does the Λ in

  $$\frac{a_1^{\gamma\gamma}}{\Lambda^4} F_{\mu\nu} F^{\mu\nu} F_{\rho\sigma} F^{\rho\sigma} + \frac{a_2^{\gamma\gamma}}{\Lambda^4} F_{\mu\nu} F^{\mu\rho} F_{\rho\sigma} F^{\sigma\nu}$$

  correspond to the mass of the particle in the loop ?

  NO! because there is a loop factor in the above diagrams

  $$\frac{a_1^{\gamma\gamma}}{\Lambda^4} \approx \frac{e^2}{16\pi^2 M^4}$$

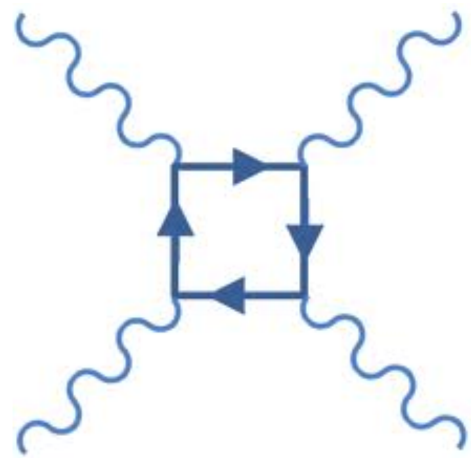

- The loop factor would be absent in non minimally coupled theories, eg. gravity where tree-level graviton exchange can give these operators without loops.

Conclusion

- For SM $\gamma\gamma WW$, 5σ discovery can be achieved with only 5/fb in diffractive photon fusion processes.
- SM $\gamma\gamma ZZ$ and $\gamma\gamma\gamma\gamma$ very hard to see because signal cross-section is small and there is a much larger background from double pomeron exchange.
- Anomalous $\gamma\gamma ZZ$ and $\gamma\gamma\gamma\gamma$ coupling limits can be improved by orders of magnitude in diffractive photon fusion processes.

Background: Double Pomeron Exchange

- pp(DPE -> γγ/ZZ)pp processes have cross section of the order of a few femtobarns.
- For pp(γγ -> γγ/ZZ)pp the invariant mass of the Z bosons can be deduced by measuring the loss of energy of the protons:

(14 TeV)^2

ZZ-invariant mass Measured by central detectors

$$W = \sqrt{\xi_1 \xi_2 s}$$

Fraction of energy lost by each proton 1 and 2.

- For DPE processes this is not true. Is this a possible way to eliminate this background?

- To measure the ZZ invariant mass we have to look at the *4l* state:

$$\sigma_{eff} = 0.56\ B(Z \to ll)^2 \sigma_{th}.$$

- However this will make cross-section less than an attobarn.